Ⓔ

Regional Correlations of V_{S30} and Velocities Averaged Over Depths Less Than and Greater Than 30 Meters

by David M. Boore, Eric M. Thompson, and Héloïse Cadet

Abstract   Using velocity profiles from sites in Japan, California, Turkey, and Europe, we find that the time-averaged shear-wave velocity to 30 m (V_{S30}), used as a proxy for site amplification in recent ground-motion prediction equations (GMPEs) and building codes, is strongly correlated with average velocities to depths less than 30 m (V_{Sz}, with z being the averaging depth). The correlations for sites in Japan (corresponding to the KiK-net network) show that V_{S30} is systematically larger for a given V_{Sz} than for profiles from the other regions. The difference largely results from the placement of the KiK-net station locations on rock and rocklike sites, whereas stations in the other regions are generally placed in urban areas underlain by sediments. Using the KiK-net velocity profiles, we provide equations relating V_{S30} to V_{Sz} for z ranging from 5 to 29 m in 1-m increments. These equations (and those for California velocity profiles given in Boore, 2004b) can be used to estimate V_{S30} from V_{Sz} for sites in which velocity profiles do not extend to 30 m. The scatter of the residuals decreases with depth, but, even for an averaging depth of 5 m, a variation in log V_{S30} of ±1 standard deviation maps into less than a 20% uncertainty in ground motions given by recent GMPEs at short periods. The sensitivity of the ground motions to V_{S30} uncertainty is considerably larger at long periods (but is less than a factor of 1.2 for averaging depths greater than about 20 m). We also find that V_{S30} is correlated with V_{Sz} for z as great as 400 m for sites of the KiK-net network, providing some justification for using V_{S30} as a site-response variable for predicting ground motions at periods for which the wavelengths far exceed 30 m.

Online Material: Estimates of V_{S30} at K-NET stations.

Introduction

The time-averaged shear-wave velocity to 30 m (V_{S30}) has a number of applications, the principal ones being its use as an explanatory variable for site effects in a number of recent ground-motion prediction equations (GMPEs; e.g., Abrahamson *et al.*, 2008) and as the basis for specifying site classes in building codes [Dobry *et al.*, 2000; Building Seismic Safety Council, 2003; Eurocode 8, 2004; American Society of Civil Engineers, 2010). V_{S30} is a simple metric that can be obtained at relatively low cost compared to more detailed descriptions of site characteristics, and it is correlated with site amplification (e.g., figure 2 in Boore *et al.*, 1994). V_{S30} cannot, of course, capture all of the physics controlling site amplification (e.g., Mucciarelli and Gallipoli, 2006; Castellaro *et al.*, 2008; Lee and Trifunac, 2010), and a significant amount of unexplained variation of ground motion remains after removing the site effect predicted by V_{S30} (as shown, for example, by Boore, 2004a, section 4.1.2, and Bragato, 2008). We recognize the limitations of V_{S30} and in this paper are not advocating its use; rather, we are

operating on the premise that it is a parameter that will continue to be used for some years.

For a number of reasons, shear-wave velocity profiles are often not available to a depth of 30 m. The reasons include technique-related limitations or environmental issues, as well as exceeding predetermined velocity thresholds or budgetary constraints. For example, shallow penetration depth from nonintrusive active-source measurements or the presence of coarse materials in seismic cone penetrometer measurements are physical limitations often encountered. To deal with situations in which a shear-wave velocity (V_S) profile does not extend to 30 m, Boore (2004b) employed various approaches for estimating V_{S30} using shear-wave velocities at shallower depths. The most straightforward approach was to use shear-wave profiles from boreholes for which the bottom depths in the profiles were greater than 30 m to derive a relation between V_{S30} and V_{Sz} for a set of depths z less than 30 m. V_{Sz} is the average V_S to depth z, computed using the equation

$$V_{Sz} = z/tt(z), \qquad (1)$$

where $tt(z)$ is the shear-wave travel time from the surface to depth z. Boore (2004b) used regression of data from boreholes in California to derive equations giving V_{S30} in terms of V_{Sz}. Other studies have used velocity profiles based on borehole measurements at Kiban-Kyoshin Network (KiK-net) sites in Japan to derive similar relations. These studies include Figini (2006) (as described in Cauzzi and Faccioli, 2008), Kanno *et al.* (2006), and Cadet and Duval (2009). In the present paper, we also use KiK-net data to establish equations from which V_{S30} can be estimated from V_{Sz}, but we provide the equations for more depths than in previous studies (e.g., Kanno *et al.* only considered $z = 20$ m, whereas our equations are at 1-m intervals from 5 to 29 m).

We expand the scope of our study to consider correlations between V_{S30} and V_{Sz} from other regions, including an extensive set of shear-wave velocity profiles from Turkey and a smaller number of profiles from other areas in Europe. The correlations for $z < 30$ m are discussed in the first part of the paper. This is followed by the use of KiK-net data to derive the equations giving V_{S30} in terms of V_{Sz}, including a separate set of equations for sites that can be assigned to the National Earthquake Hazards Reduction Program (NEHRP) class E ($V_{S30} < 180$ m/s) based on *a priori* information. This section is followed by one that considers the sensitivity of ground motions from several recent GMPEs to the variability in V_{S30} estimated from V_{Sz}, as well as comments on applying the equations from the KiK-net profiles to estimate V_{S30} at Kyoshin Network (K-NET) stations in Japan, for which velocity profiles do not extend beyond 20 m. In the final section we consider correlations of V_{S30} with shear-wave velocities averaged over depths exceeding 30 m.

Correlations of V_{Sz} and V_{S30} for $z < 30$ m: Regional Similarities and Differences

We consider correlations of V_{S30} and V_{Sz} from shear-wave velocity profiles derived from data in Japan, California, Turkey, and other parts of Europe. The velocity profiles at the stations in Japan were derived from measurements in boreholes drilled at sites of the KiK-net network. Similarly, the profiles in California are from a compendium of borehole measurements (Boore, 2003b). In contrast, the profiles in Turkey were derived from the noninvasive multichannel analysis of surface waves method at sites of the Turkish National Strong-Motion network (Sandıkkaya *et al.*, 2010).

The Data and Resources section gives the sources of the profiles from Japan, California, and Turkey. The V_{Sz} values for other sites in Europe are from table 4 in Cadet and Duval (2009); these profiles were computed from a variety of invasive and noninvasive methods (see Boore, 2006, for a discussion of the methods). We checked the velocity profiles for problems such as missing values, depths that did not increase monotonically, etc. The most extensive set of profiles are from the KiK-net network; of the 657 profiles, 19 were eliminated because of null or zero entries for the velocities. Note that no thickness is given for the lowest velocity in the KiK-net profile data files. The depth to the bottom of the penultimate velocity in each profile is often much less than the installation depth, and we were unsure whether to assume that the lowest layer in each profile had a constant velocity over a thickness of tens to hundreds of meters. Personal communications from Y. Fukushima and H. Kawase (May 2011) and the pdf files downloadable from the KiK-net Web site (containing geologic logs and velocity profiles; see Data and Resources) confirm that the lowest velocity should be assumed to extend to the installation depth. We have made that assumption in our analysis, and this results in 638 shear-wave velocity profiles extending to at least 99 m. Average velocities V_{S30} and V_{Sz} for the Japan, California, and Turkey datasets were then computed for a series of depths using equation (1) (that computation had already been done by Cadet and Duval for the Europe dataset). The number of profiles for each dataset are given in Table 1.

The correlations of V_{S30} and V_{Sz} are shown in Figure 1 for four depths (5, 10, 15, and 20 m). Pearson correlation coefficients for the KiK-net values are given in the graph legends (the correlation coefficients for all datasets are given in Table 1 for the four depths). Both visually and from the correlation coefficients, it is obvious that there is a strong correlation between V_{S30} and V_{Sz}, even for z as small as 5 m. The correlations for California, Turkey, and Europe are similar to one another, while V_{S30} for Japan is systematically higher than from the other regions for a given V_{Sz}. This is seen most clearly for small values of z (as z approaches 30 m, the correlations must approach unity, and there will be no regional differences).

Although there are obvious differences in the correlations between Japan and the other regions, the correlations themselves do not provide information about the distributions of the V_{Sz} values. We discuss here those values from Japan, California, and Turkey. As shown by the quantile–quantile

Table 1

Pearson Correlation Coefficients (r) between V_{Sz} and $\log V_{S30}$ for Four Depths (z)

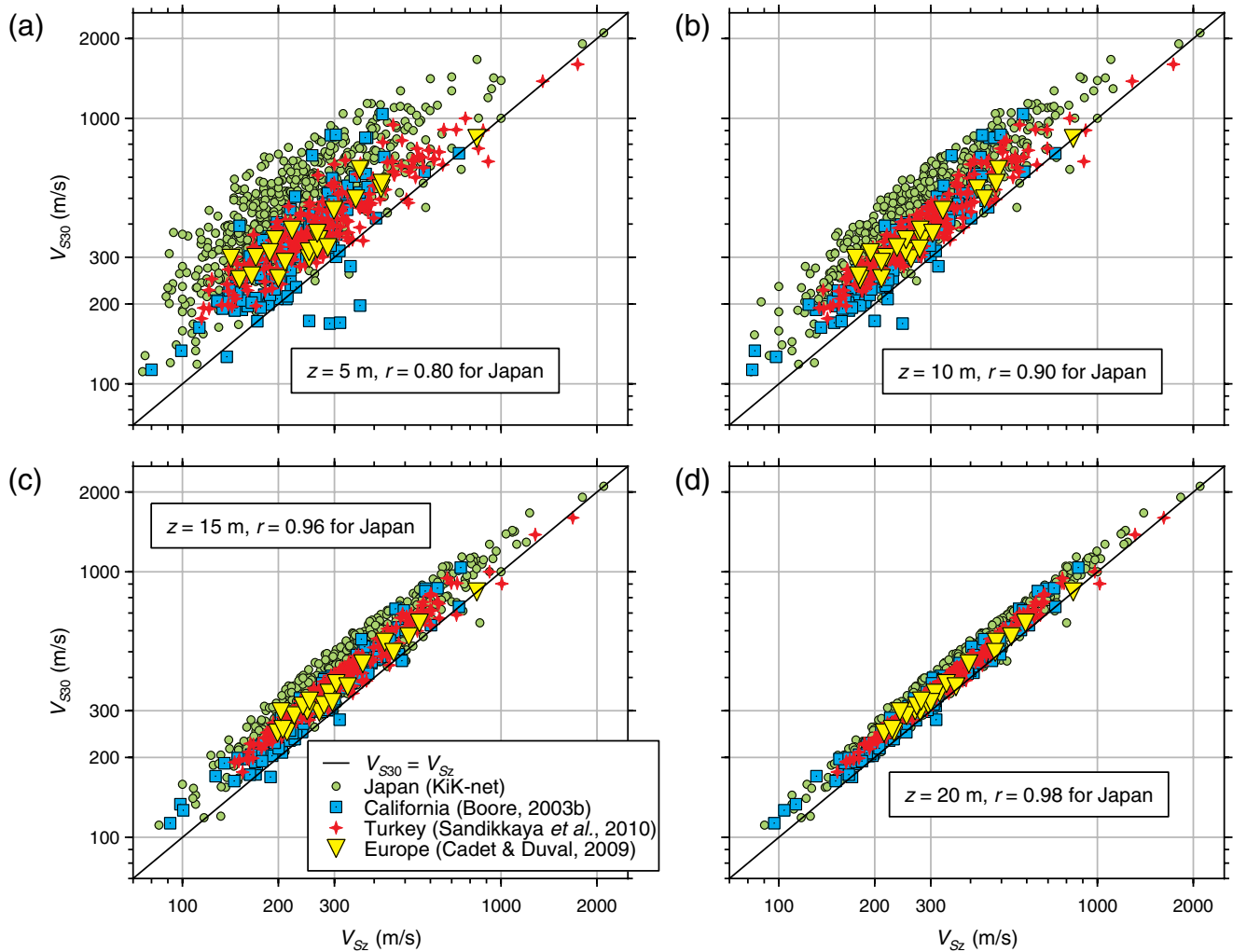| Dataset	Number of Profiles, n	r ($z = 5$ m)	r ($z = 10$ m)	r ($z = 15$ m)	r ($z = 20$ m)
Japan (KiK-net)	638	0.80	0.90	0.96	0.98
California	135	0.75	0.92	0.97	0.99
Turkey	228	0.91	0.95	0.98	0.99
Europe	21	0.90	0.96	0.98	0.99

Figure 1. Correlation of V_{S30} and V_{Sz} from shear-wave velocity profiles from Japan, California, Turkey, and a mix of locations in Europe for averaging depths z of 5, 10, 15, and 20 m. The Pearson correlation coefficient r between $\log V_{Sz}$ and $\log V_{S30}$ for the Japan dataset is given in the comment box for each graph. (Table 1 contains r for all datasets.) The color version of this figure is available only in the electronic edition.

plots in Figure 2 for the KiK-net data, the V_{S30} observations closely follow a log-normal distribution. Although not shown here, this is true for other values of averaging depth, and for this reason we work primarily with $\log V_{Sz}$ in the rest of this paper. Histograms of $\log V_{S5}$ and $\log V_{S30}$ for Japan, California, and Turkey are given in Figure 3 (there are too few data for the Europe dataset to make meaningful histograms). These histograms show that V_{S5} is similar for the three regions (although those from Turkey are somewhat larger), whereas the V_{S30} values from California are systematically lower than those from Japan, with those from Turkey tending to be between those from California and Japan (although there is considerable overlap in the velocities). The implication is that the surface sediments are similar at the sites for the three regions (particularly for California and Japan) but that the gradient of velocity with depth is greater for Japan than California.

The reason for the systematic differences in the shear-wave velocities beneath the California and Japan borehole

sites may be due to the different criteria used in siting the Japanese and the California strong-motion stations at which the borehole measurements were made. The KiK-net stations in Japan are located on a nominally uniform grid, which means that a number of stations are in valleys in hilly terrain with shallow sediments over rock. In contrast, the California stations are predominately in urban areas, such as the Los Angeles and San Francisco areas, which are located within broad areas of low topographic relief, underlain by sedimentary basins. Support for a difference in the siting of the boreholes comes from the histograms of topographic slopes shown in Figure 4. These slopes were computed from 30-arc-sec digital elevation models, as employed by Shake-Map for estimating site response (Wald and Allen, 2007; Allen and Wald, 2009). Clearly, the slopes at the California borehole sites are systematically lower than those at the sites in Japan, indicating the tendency for the Japanese stations to be sited on stiffer soils or rock.
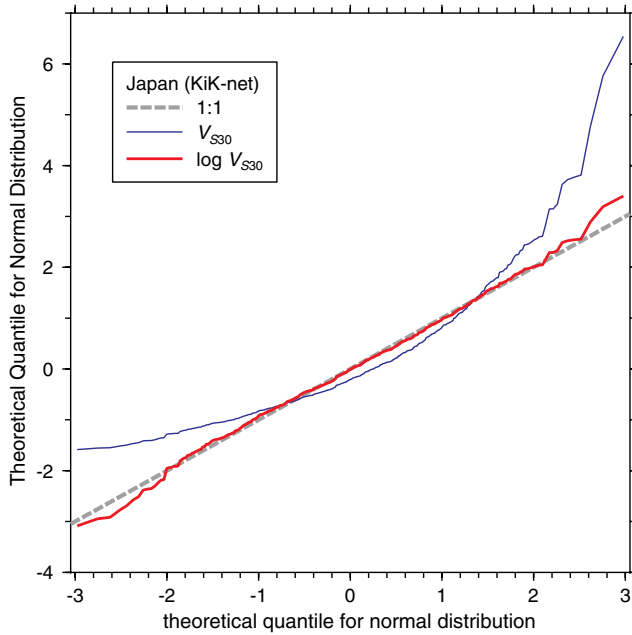
Figure 2. Quantile–quantile plots for V_{S30} and $\log V_{S30}$ from the KiK-net profiles. An observed quantile is the standardized residual of the sorted data (i.e., the difference between a sorted value and the mean of all values divided by the standard deviation of the values). Note: We plot lines rather than individual points in order to show detail in the midrange of quantiles, where there are so many points that detail would be lost unless tiny symbols were used. The color version of this figure is available only in the electronic edition.

Equations for V_{S30} as a Function of V_{Sz} from KiK-net Profiles

The regional differences in the velocity structure illustrated in Figures 3 and 4 demonstrate that the empirical relationships developed by Boore (2004b) may not be appropriate for the sites in Japan. Following Boore (2004b), who used data from California, we derive equations for V_{S30} in terms of V_{Sz} for Japan by using the KiK-net velocity profiles. Kanno *et al.* (2006), Cauzzi and Faccioli (2008), and Cadet and Duval (2009) also derived equations giving V_{S30} in terms of V_{Sz} from KiK-net data, but their studies were limited to a more restricted set of depths than in this study (e.g., Kanno *et al.* only considered $z = 20$ m, and Cadet and Duval provided equations for depths of 5, 10, and 20 m). We provide equations at 1-m intervals, and we also give equations that can be used if sites can be assigned to NEHRP class E on the basis of *a priori* information. We do not give equations for the Turkey velocity profiles because the correlations between V_{S30} and V_{Sz} are similar to those from California, and the equations for California are given in Boore (2004b).

We made many plots of V_{S30} versus V_{Sz} for the KiK-net data using different functional forms to fit the data, and we considered V_{Sz}, $\log V_{Sz}$, and slowness ($1/V_{Sz}$) as the predictor variables in the equations. We finally decided that the best predictor variable was $\log V_{Sz}$. For application to sites for which nothing is known except for the velocity profile, it

is appropriate to use a single equation relating $\log V_{S30}$ and $\log V_{Sz}$. We found that a second-order polynomial was sufficient to model the data (a cubic led to an insignificant decrease in the variance of the residuals of the observations about the regression line). The following equation was used for the fit:

$$\log V_{S30} = c_0 + c_1 \log V_{Sz} + c_2 (\log V_{Sz})^2, \quad (2)$$

with coefficients and the standard deviation of the residuals to the fit (σ_{RES}) in Table 2. The data are shown in Figure 5, for $z = 10$ m, along with the regression fit. Figure 6 shows the standard deviation of the observations about the regression fit as a function of averaging depth z. As expected, the standard deviation decreases monotonically to zero as z approaches 30 m.

Note that for small values of V_{S10}, the observed values of V_{S30} are systematically lower than those predicted from the regression fits (Figure 5). Many of these points correspond to sites that would fall into NEHRP class E ($V_{S30} < 180$ m/s), as shown by the different symbols. (In the NEHRP code, class E can also be assigned to sites on the basis of blow counts or shear strength, even if $V_{S30} > 180$ m/s; our assignments are based strictly on V_{S30}). Although not shown here, this bias tends to disappear for greater averaging depths. We think that class E can be assigned fairly reliably from visual inspection of the sites (such sites are often underlain by muds and silts, as occur near estuaries and river deltas). In view of the uniqueness of class E sites, we derived regression equations for which all sites (including class E) were used to define the trend with V_{Sz}, but a dummy variable was used for class E sites (this corresponding to a constant shift of $\log V_{S30}$ relative to the other classes). The following equation was used for the fit:

$$\log V_{S30} = c_{oE}\delta_E + c_0 + c_1 \log V_{Sz} + c_2 (\log V_{Sz})^2, \quad (3)$$

where $\delta_E = 1$ for class E and $\delta_E = 0$ otherwise, with coefficients and the standard deviation of the residuals to the fit listed in Table 3. The fit to the data is shown in Figure 5. Although there is a only a small reduction in the standard deviation of the overall residuals about the fit when class E sites are considered separately (4% at most), the V_{S30} values for class E sites are systematically lower, by about a factor of 0.6 for $z = 5$ m (and 0.7 for $z = 10$ m), than would be estimated from equation 2.

Using the Equations for V_{S30} as a Function of V_{Sz}

The Impact of Uncertainty in Predicted V_{S30} on Ground-Motion Estimates

As mentioned earlier, one of the main uses of V_{S30} is for characterizing site response in GMPEs. Even though there is a strong correlation between V_{S30} and V_{Sz}, the variability of individual values of V_{S30} for a given value of V_{Sz} can have an impact on site-specific predictions of ground motions if the
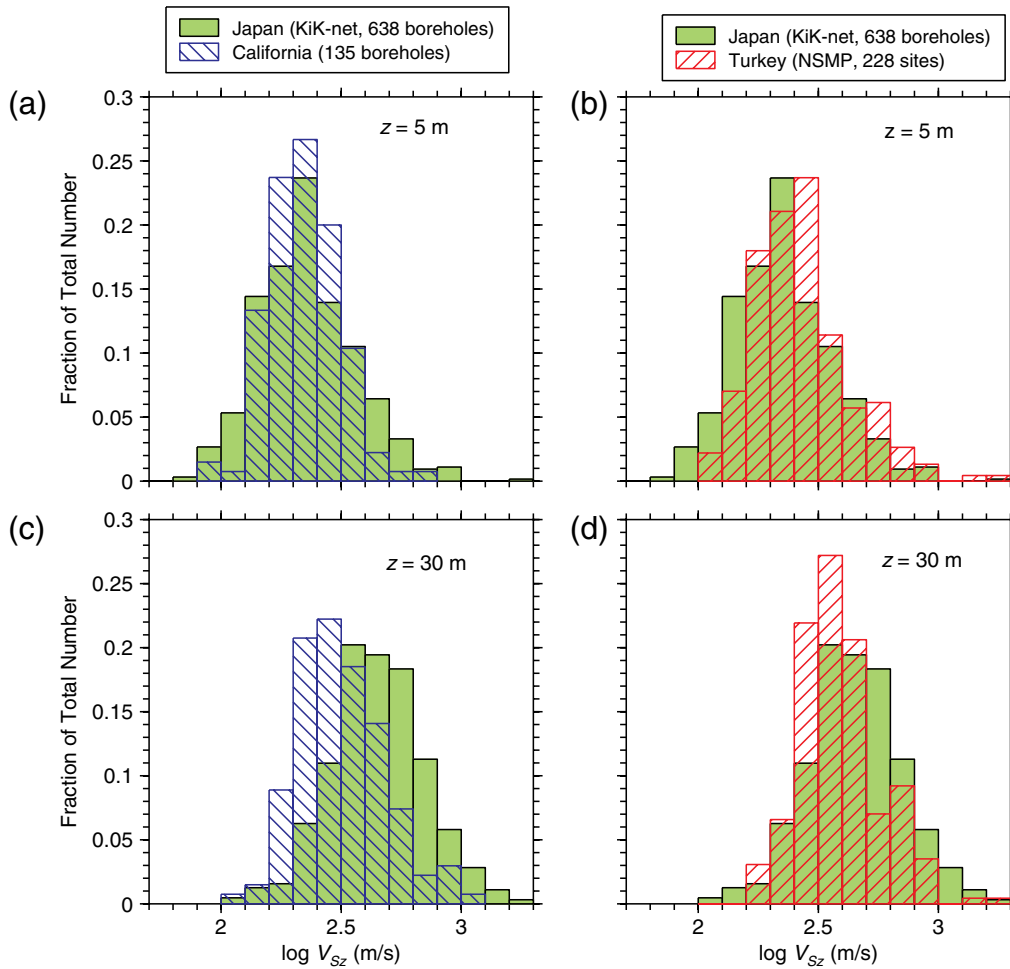
Figure 3. Histograms of $\log V_{S5}$ (top row) and $\log V_{S30}$ (bottom row) for shear-wave velocity profiles from three regions. Only profiles extending to depths of at least 30 m are used in this figure. The color version of this figure is available only in the electronic edition.

equations in Tables 2 or 3 are used to estimate V_{S30} at sites for which velocity profiles do not extend to 30 m (as for stations of the K-NET network, discussed in the Application to K-NET Stations section). We are not concerned with errors in the velocity profiles obtained from the borehole measurements (e.g., Moss, 2008) or the effect of those errors on GMPE development (e.g., Moss, 2011) but rather with the impact of uncertainties in V_{S30} when used with previously developed GMPEs. The extrapolated values of V_{S30} will be of little use if their uncertainty is so large that ground-motion estimates using the extrapolated values are also highly uncertain. To evaluate the impact of the uncertainty in estimates of V_{S30} on predicted ground motions, we use some recent GMPEs that use V_{S30} as a site variable.

The simplest relation between a ground-motion parameter Y and V_{S30} was introduced by Joyner and Fumal (1985):

$$\log Y \propto b_{LIN} \log V_{S30}. \qquad (4)$$

This equation was used in the GMPEs of Boore *et al.* (1994, 1997), where typical values of b_{LIN} range from -0.23 to -0.75, depending on period (e.g., Boore and Atkinson,

2008). From this equation, the relation between the standard deviations of predicted motions and V_{S30} is given by

$$\sigma_{\log Y} = |b_{LIN}|\sigma_{\log V_{S30}}. \qquad (5)$$

Taking the largest value of b_{LIN} in Boore and Atkinson (-0.75 for a period of 4 s) and the largest σ_{RES} in Figure 6 (0.12, corresponding to a factor of 1.3) for $\sigma_{\log V_{S30}}$ gives $\sigma_{\log Y} = 0.09$ (a factor of 1.2). This is a relatively small uncertainty, given that we have chosen a σ value to maximize the uncertainty. However, this estimate does not reflect the more complex role of V_{S30} in a number of recent GMPEs, in which V_{S30} appears in nonlinear amplification terms as well as implicitly in sediment-depth factors (through correlations of V_{S30} and sediment depth if the latter are not available when evaluating the GMPEs—generally, lower values of V_{S30} are associated with deeper depths of sedimentary deposits. Examples of such correlations are equation 17 in Abrahamson and Silva, 2008 and equation 1 in Chiou and Youngs, 2008).
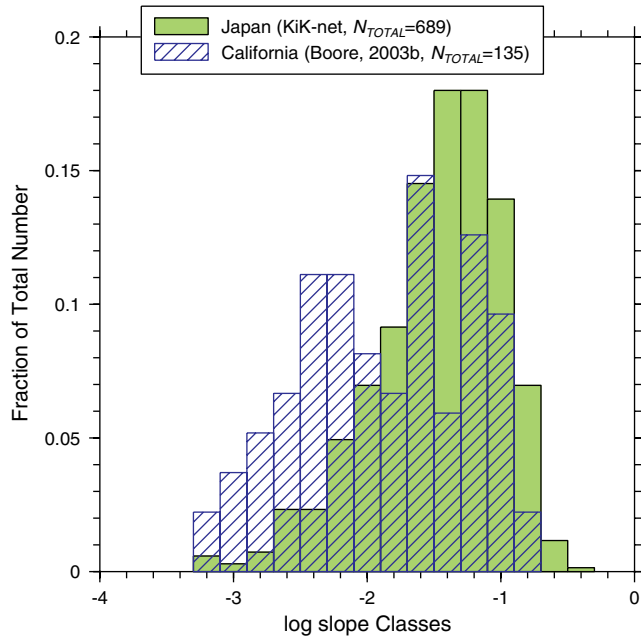
Figure 4. Histogram of slopes (m/m, as a decimal quantity, not a percent) from 30-arc-sec digital elevation models at sites in California and Japan from which the velocity profiles were obtained. The color version of this figure is available only in the electronic edition.

To give a more complete view of the sensitivity of ground motions to the uncertainty in V_{S30}, we used four recent GMPEs derived as part of the Pacific Earthquake Engineering Research Institute's Next Generation Attenuation (PEER NGA) project (the references for the specific GMPEs are given in the caption to Figure 7) for an earthquake magnitude of 7, a vertical strike-slip fault, and Joyner–Boore distance (R_{JB}) of 20 km. We evaluated the GMPEs for values of V_{S30} corresponding to ± 1 standard deviation of 0.12 in the predicted values of log V_{S30} around V_{S30} values of 300 and 600 m/s. The standard deviation of 0.12 is close to the maximum standard deviation found in the regression fits (for a 5-m averaging depth; Fig. 6). Figure 7 gives ratios of predicted pseudoabsolute response spectral acceleration (PSA) for the low and high values of V_{S30} about each central value; the actual values of V_{S30} are indicated in the figure, and the ratios of V_{S30} are shown by the horizontal lines to provide a reference for the relative uncertainty in PSA and V_{S30}, expressed as multiplicative factors. We used the relations between V_{S30} and sediment depth recommended by each GMPE developer (only the Boore and Atkinson GMPEs do not involve sediment depth). To give an idea of how the results would change for a smaller uncertainty, in the left graph we show results for two GMPEs for an uncertainty of 0.04 in log V_{S30}, the value for a depth near 20 m (see Fig. 6 and

Table 2
Coefficients of Equation (2) in Text, Relating log V_{S30} and log V_{Sz} for KiK-Net Data, without Regard to Site Class

| Depth, z (m)	Coefficients of Equation (2)			Standard Deviation of Residuals, σ_{RES}
	c_0	c_1	c_2	
5	2.046×10^{-1}	1.318×10^{0}	-1.174×10^{-1}	0.119
6	-6.072×10^{-2}	1.482×10^{0}	-1.423×10^{-1}	0.111
7	-2.744×10^{-1}	1.607×10^{0}	-1.600×10^{-1}	0.103
8	-3.723×10^{-1}	1.649×10^{0}	-1.634×10^{-1}	0.097
9	-4.941×10^{-1}	1.707×10^{0}	-1.692×10^{-1}	0.090
10	-5.438×10^{-1}	1.715×10^{0}	-1.667×10^{-1}	0.084
11	-6.006×10^{-1}	1.727×10^{0}	-1.649×10^{-1}	0.078
12	-6.082×10^{-1}	1.707×10^{0}	-1.576×10^{-1}	0.072
13	-6.322×10^{-1}	1.698×10^{0}	-1.524×10^{-1}	0.067
14	-6.118×10^{-1}	1.659×10^{0}	-1.421×10^{-1}	0.062
15	-5.780×10^{-1}	1.611×10^{0}	-1.303×10^{-1}	0.056
16	-5.430×10^{-1}	1.565×10^{0}	-1.193×10^{-1}	0.052
17	-5.282×10^{-1}	1.535×10^{0}	-1.115×10^{-1}	0.047
18	-4.960×10^{-1}	1.494×10^{0}	-1.020×10^{-1}	0.043
19	-4.552×10^{-1}	1.447×10^{0}	-9.156×10^{-2}	0.038
20	-4.059×10^{-1}	1.396×10^{0}	-8.064×10^{-2}	0.035
21	-3.827×10^{-1}	1.365×10^{0}	-7.338×10^{-2}	0.030
22	-3.531×10^{-1}	1.331×10^{0}	-6.585×10^{-2}	0.027
23	-3.158×10^{-1}	1.291×10^{0}	-5.751×10^{-2}	0.023
24	-2.736×10^{-1}	1.250×10^{0}	-4.896×10^{-2}	0.019
25	-2.227×10^{-1}	1.202×10^{0}	-3.943×10^{-2}	0.016
26	-1.768×10^{-1}	1.159×10^{0}	-3.087×10^{-2}	0.013
27	-1.349×10^{-1}	1.120×10^{0}	-2.310×10^{-2}	0.009
28	-9.038×10^{-2}	1.080×10^{0}	-1.527×10^{-2}	0.006
29	-4.612×10^{-2}	1.040×10^{0}	-7.618×10^{-3}	0.003
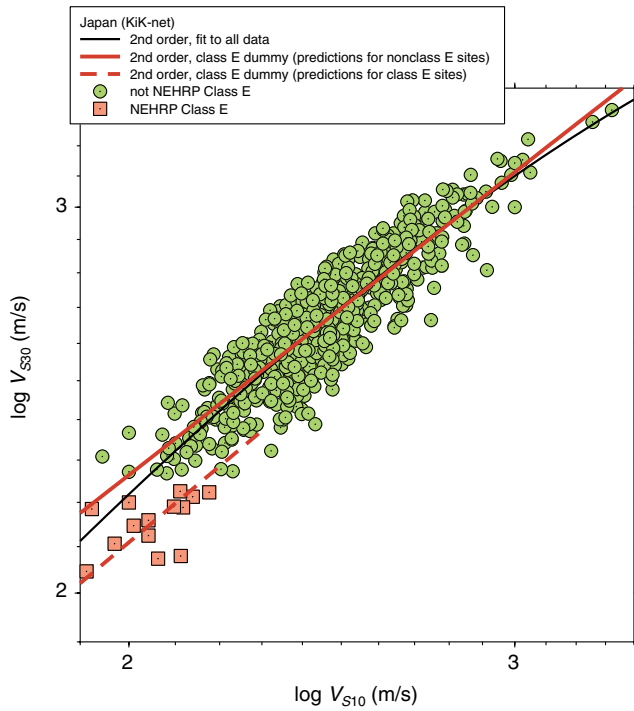
Figure 5. Correlation of $\log V_{S30}$ and $\log V_{S10}$ from KiK-net data. Also identified are the NEHRP class E sites (based on the known value of V_{S30}) and the polynomial fits to all of the data and to all of the data with a dummy variable for class E sites (see text). The color version of this figure is available only in the electronic edition.
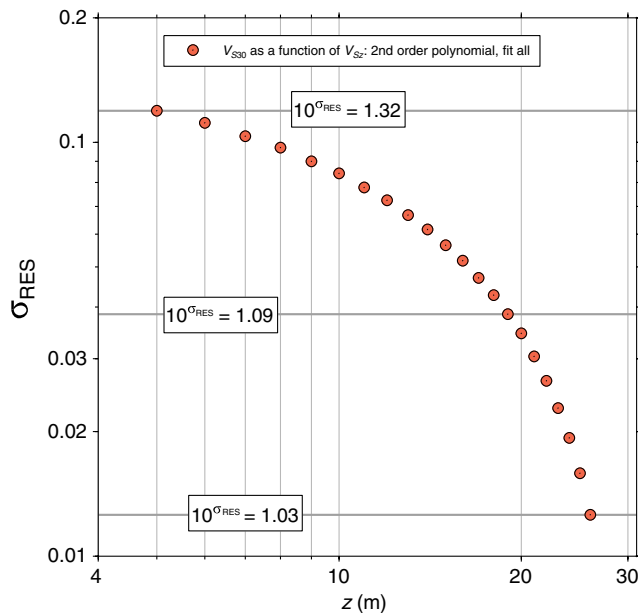

Figure 6. The depth dependence of the standard deviation of $\log V_{S30}$ residuals relative to the fit of a second-order polynomial in $\log V_{S_z}$ for depths less than 30 m. (A third-order polynomial gave similar results.) For the convenience of the reader, the equivalences of the standard deviations to multiplicative factors are shown by the horizontal lines. The color version of this figure is available only in the electronic edition.

Table 2). Figure 7 also shows the ratio of predicted response spectra using the linear amplification given by equation (4), with b_{LIN} taken from Boore and Atkinson (2008, table 3, which are modified from Choi and Stewart, 2005). The difference in the response spectral ratios for the purely linear site response and the site response of the GMPEs is largest for $V_{S30} = 300$ m/s (left graph). Note that the ratios for most of the GMPEs approach unity for periods less than about 0.2 s for $V_{S30} = 300$ m/s, but this is not true for $V_{S30} = 600$ m/s. We think that this is a coincidence in which the larger linear amplification at the lower values of V_{S30} is being offset by greater nonlinear deamplification.

For periods less than about 2 s, Figure 7 shows that the uncertainty in the ground motions is significantly less than the uncertainty in V_{S30} for both median values of V_{S30}. For example, the uncertainty factor of 1.74 in V_{S30} (corresponding to an averaging depth of 5 m) results in less than a factor of 1.2 uncertainty in ground-motion intensity for periods less than 0.2–0.4 s. Because of the muting effect of soil nonlinearity discussed previously in this paper, at short periods equation (5) can be used to give a quick (and conservative) estimate of the uncertainties for situations not included in Figure 7 (e.g., different magnitudes, distances, and V_{S30} values). As an example, consider an uncertainty in V_{S30} of a factor of 1.5 for $\pm\sigma_{\log V_{S30}}$, analogous to the V_{S30} ratios in Figure 7 of 1.73. This ratio equates to $\sigma_{\log V_{S30}} = 0.09$, which is close to σ_{RES} for a depth of 10 m (see Table 2). For periods less than about 0.2 s, $|b_{LIN}|$ is close to 0.3 (Boore and Atkinson, 2008). The uncertainty in Y is then a factor of about $(1.5)^{0.3} = 1.13$.

The V_{S30} sensitivity of ground motions predicted from the NGA GMPEs increases with period (Fig. 7). This is due to at least three factors: (1) the site response generally increases as period increases (e.g., linear amplification $|b_{LIN}|$ increases with period), (2) the longer-period motions are more sensitive to sediment depth than are the motions at shorter periods, and (3) the muting effects of soil nonlinearity are less important at long periods than at short periods. We caution that these conclusions are based on the NGA GMPEs and may not be a global feature—certainly at sufficiently long period the ground motions will no longer be sensitive to surficial geology, and the site response will then decrease toward unity as period increases (e.g., starting at some period, $|b_{LIN}|$ should begin to decrease for linear amplification). The results in Figure 7 suggest that considerable uncertainty exists in predicting ground motions at long periods when using V_{S30} values estimated from velocity profiles that only extend to 5 or 10 m. Because of the increasing accuracy of V_{S30} for greater values of the averaging depth z, however, the uncertainties in predicted motions due to the estimation of V_{S30} will obviously decrease with increasing maximum depth of the velocity profile (e.g., for a depth of about 20 m, the uncertainties in predicted motion will generally be less than 20% for all periods).

Table 3
Coefficients of Equation (3) in Text, Relating $\log V_{S30}$ and $\log V_{Sz}$ for KiK-Net Data, with Class E as a Dummy Variable

Depth, z (m)	Coefficients of Equation (3)				Standard Deviation of Residuals, σ_{RES}
	c_{0E}	c_0	c_1	c_2	
5	-2.549×10^{-1}	1.146×10^{0}	5.810×10^{-1}	2.573×10^{-2}	0.114
6	-2.316×10^{-1}	8.962×10^{-1}	7.366×10^{-1}	1.817×10^{-3}	0.107
7	-2.077×10^{-1}	6.788×10^{-1}	8.675×10^{-1}	-1.782×10^{-2}	0.100
8	-1.906×10^{-1}	5.684×10^{-1}	9.224×10^{-1}	-2.416×10^{-2}	0.094
9	-1.702×10^{-1}	4.219×10^{-1}	1.002×10^{0}	-3.468×10^{-2}	0.087
10	-1.547×10^{-1}	3.462×10^{-1}	1.033×10^{0}	-3.680×10^{-2}	0.082
11	-1.362×10^{-1}	2.453×10^{-1}	1.081×10^{0}	-4.223×10^{-2}	0.076
12	-1.214×10^{-1}	1.932×10^{-1}	1.097×10^{0}	-4.211×10^{-2}	0.071
13	-1.021×10^{-1}	8.882×10^{-2}	1.151×10^{0}	-4.915×10^{-2}	0.066
14	-8.610×10^{-2}	2.964×10^{-2}	1.174×10^{0}	-5.075×10^{-2}	0.061
15	-7.132×10^{-2}	-2.178×10^{-2}	1.191×10^{0}	-5.150×10^{-2}	0.056
16	-5.981×10^{-2}	-5.916×10^{-2}	1.201×10^{0}	-5.115×10^{-2}	0.051
17	-4.760×10^{-2}	-1.287×10^{-1}	1.235×10^{0}	-5.555×10^{-2}	0.047
18	-3.740×10^{-2}	-1.725×10^{-1}	1.252×10^{0}	-5.697×10^{-2}	0.043
19	-2.874×10^{-2}	-1.992×10^{-1}	1.256×10^{0}	-5.610×10^{-2}	0.038
20	-2.161×10^{-2}	-2.088×10^{-1}	1.250×10^{0}	-5.346×10^{-2}	0.034
21	-1.581×10^{-2}	-2.353×10^{-1}	1.255×10^{0}	-5.317×10^{-2}	0.030
22	-1.125×10^{-2}	-2.462×10^{-1}	1.251×10^{0}	-5.127×10^{-2}	0.027
23	-7.740×10^{-3}	-2.409×10^{-1}	1.236×10^{0}	-4.735×10^{-2}	0.023
24	-5.146×10^{-3}	-2.231×10^{-1}	1.212×10^{0}	-4.213×10^{-2}	0.019
25	-2.991×10^{-3}	-1.929×10^{-1}	1.180×10^{0}	-3.543×10^{-2}	0.016
26	-2.026×10^{-3}	-1.564×10^{-1}	1.144×10^{0}	-2.814×10^{-2}	0.013
27	-7.695×10^{-4}	-1.270×10^{-1}	1.114×10^{0}	-2.205×10^{-2}	0.009
28	-1.078×10^{-4}	-8.924×10^{-2}	1.079×10^{0}	-1.512×10^{-2}	0.006
29	2.384×10^{-4}	-4.862×10^{-2}	1.042×10^{0}	-7.949×10^{-3}	0.003

Application to K-NET Stations

In Japan there are two large networks of strong-motion stations: K-NET and KiK-net (Kinoshita, 1998; Okada *et al.*, 2004). Both the K-NET and KiK-net networks are spread more-or-less uniformly throughout Japan, with an average station spacing of about 25 km for K-NET and somewhat more for KiK-net; K-NET has surface sensors, whereas KiK-net has both surface and borehole sensors. Borehole velocity measurements have been made at each site for both networks. As we have seen, the velocity profiles at KiK-net stations are available to depths well in excess of 30 m (the profiles range in total thickness from 99 to 2003 m, with concentrations at 100- and 200-m depths). In contrast, the velocity profiles for the K-NET stations extend no deeper than 20 m, with a strongly bimodal distribution of maximum depths (z_{max}): z_{max} equals 10 m for 36% of profiles and 20 m for 46% of profiles. However, there are more K-NET stations (1042) than KiK-net stations (689), and more than 7600 earthquakes have been recorded on K-NET stations (the numbers of stations are from information downloaded in August 2010). For this reason, it is useful to estimate V_{S30} at the K-NET sites from the V_{Sz} values corresponding to the maximum profile depth at each site. This is most conveniently done using equations relating V_{S30} to V_{Sz}. To do this, it is tempting to use the equations from the KiK-net profiles given in Table 2. An important assumption in doing so,

however, is that the velocity profiles beneath K-NET and KiK-net sites are similar. Maps showing the spatial distributions of the stations indicate that both networks appear to be uniformly distributed across a similar geographic extent, thus implying that the velocity profiles sampled by each network is similar. Okada *et al.* (2004, p. xxiii), however, notes that there were different siting criteria for the two networks: "Since K-NET was planned to record strong motion at typical inhabitant area, the station usually locates at soil site, whereas KiK-net station is located at rock site if available, because it is colocated to the Hi-net aimed for microearthquake observation." The results of the different siting criteria are apparent in histograms of V_{Sz} values for depths of 10 and 20 m (the two most common maximum depths for the K-NET velocity profiles). Figure 8 shows histograms of V_{S10} and V_{S20} for the K-NET, KiK-net, and California velocity profiles. As shown in the lower left graph, the V_{S20} values for K-NET (for which no profiles exceed 20 m) are clearly lower on average than the KiK-net values. This is consistent with the Okada *et al.* (2004) statement that K-NET and KiK-net stations are located on soil and rock sites, respectively. Inconsistent with this, however, is that the V_{S10} values for the K-NET velocity profiles with a maximum depth of 10 m are clearly higher on average than the V_{S20} values for K-NET (for which no profiles exceed 20 m; compare the top and bottom graphs in Figure 8). This suggests that a number
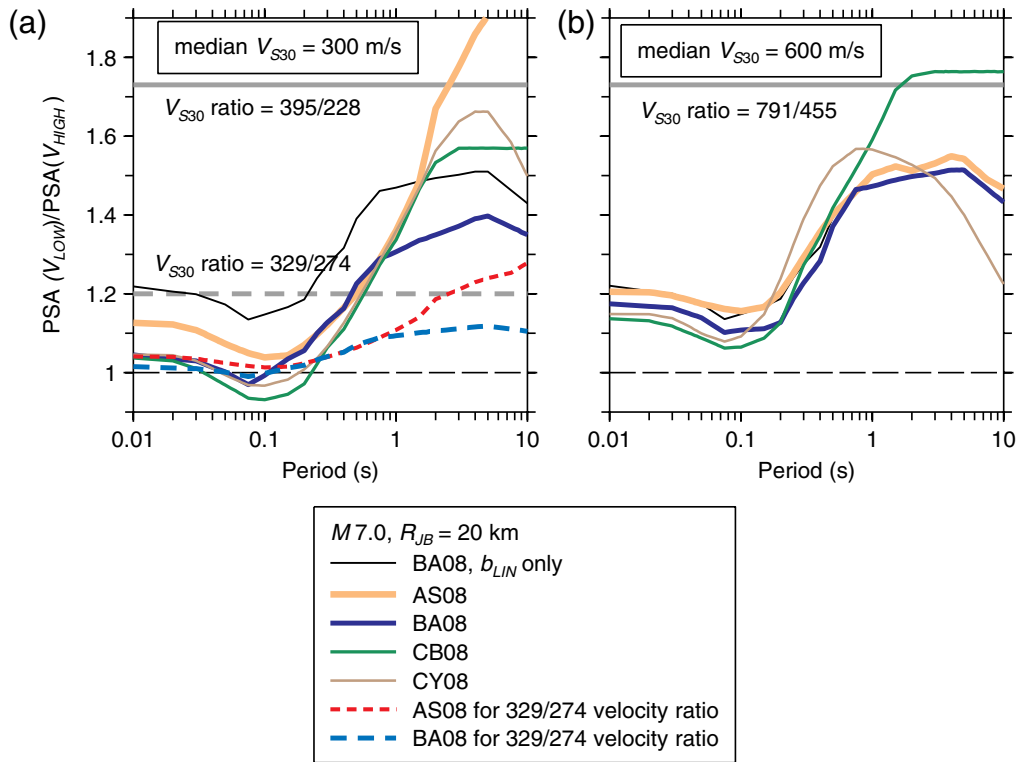
Figure 7. Ratio of pseudoabsolute response spectral acceleration (PSA) from the Abrahamson and Silva (2008: AS08), Boore and Atkinson (2008: BA08), Campbell and Bozorgnia (2008: CB08), and Chiou and Youngs (2008: CY08) ground-motion prediction equations for ranges of V_{S30} centered about 300 and 600 m/s. Also shown is the ratio of response spectra using only the linear amplifications of BA08. The ranges correspond to the log of the center velocity ± 0.12 log units (except for the lower ratios of AS08 and BA08 in the left graph, which correspond to ± 0.04 log units). The ratio of high-to-low velocities is the same in all graphs, as shown by the horizontal lines (the high and low values are given for each ratio); these lines provide a reference for the relative uncertainty in PSA and V_{S30}, expressed as multiplicative factors. The color version of this figure is available only in the electronic edition.

of K-NET sites are located on rocklike sites. The different distributions of V_{S10} and V_{S20} for K-NET, as well as the strongly bimodal distribution of z_{max}, is consistent with the procedure used in the velocity measurements at K-NET sites, in which drilling proceeded until relatively hard materials were encountered (S. Kinoshita, personal commun., 2002). Additionally, the distribution of V_{S10} for K-NET is more similar to that from KiK-net than from California, but the opposite is the case for V_{S20}. This suggests that the KiK-net equations in Table 2 should be used to estimate V_{S30} at those K-NET sites for which the maximum depth of the velocity profile equals 10 m, and, paradoxically, the California equations in Boore (2004b) might be better for K-NET sites with $z_{max} = 20$ m. Ⓔ In the electronic supplement to this paper, we give estimates of V_{S30} for K-NET sites, assuming that V_{max} continues to 30 m (i.e., a constant-velocity extrapolation). We also give estimates from both sets of equations, as well as from a linear weighted combination of the log V_{Sz} estimates from the KiK-net and the California equations. The latter are our preferred estimates. The weighting equals unity for the KiK-net estimates if z_{max} is less than or equal to 10 m, unity for the California estimates if z_{max} is equal to

20 m, with linear weighting between these two values for z_{max} between 10 and 20 m.

Correlations of V_{S30} with V_{Sz} for $z > 30$ m

One criticism of V_{S30} as a site-response parameter in GMPEs is that the averaging depth of 30 m is too shallow to reflect the velocity structure that can affect periods longer than a few tenths of a second. The basis for this is shown in Figure 9, which shows the depth corresponding to one-quarter of a wavelength for various periods. Each symbol in the plot represents a particular velocity profile. For each profile the equation

$$T = 4z/V_{Sz}, \qquad (6)$$

where $z = z_{max}$, was used to compute the period T for which z_{max} is one-quarter of a wavelength. One interpretation of Figure 9 is that it gives the minimum required depth of the profile such that the depth is a quarter wavelength at the specified period. Note that there is considerable scatter of the depths for a given period due to the different velocity profiles [e.g., the two California points at about 3.5 s are from boreholes
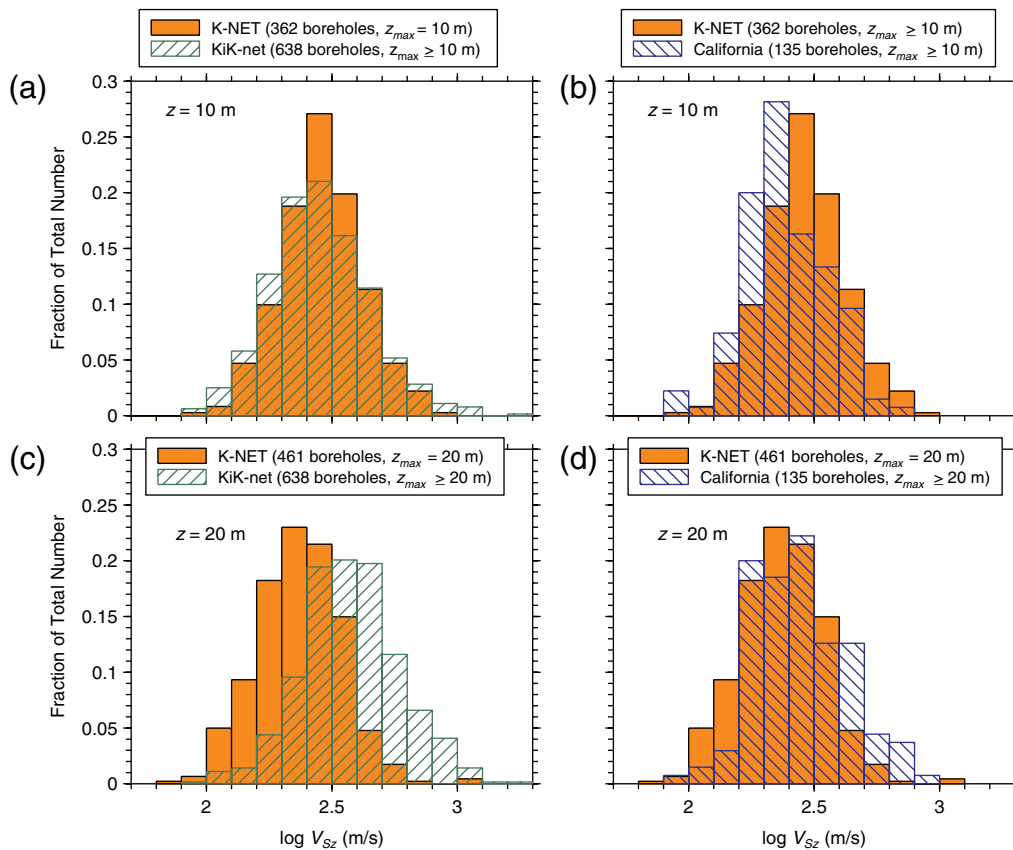
Figure 8. Histograms of $\log V_{S10}$ and $\log V_{S20}$ for shear-wave velocity profiles from K-NET, KiK-net, and California, for profiles with z_{max} as indicated. The color version of this figure is available only in the electronic edition.

penetrating very different geologic materials, the Varian hole (Daley and McEvilly, 1990) being in Tertiary rock near Parkfield, California, and the Long Beach Water Treatment hole being in the Los Angeles Basin (see Data and Resources for ROSRINE velocity profiles)]. Assuming that site amplification is controlled by velocities within one-quarter wavelength of the surface (e.g., Joyner *et al.*, 1981; Day, 1996; Boore, 2003a), the figure also can be used to estimate the minimum depth required to provide site amplification information for a given period. For example, it would seem that profiles must extend to at least 100 m if they are to be used to estimate amplifications at periods as long as 2 s. Another interpretation of Figure 9 is that velocities known only to 30 m are relevant for site amplifications at periods less than 1 s (being most useful for periods between about 0.1– 0.6 s).

Suggestions have been made that more accurate ground-motion predictions can be obtained if site classifications are based on depths commensurate with the period of ground motion being estimated (e.g., Joyner *et al.*, 1981; Douglas *et al.*, 2009). Implied in this suggestion is that V_{S30} does not correlate well with V_{Sz} for depths greater than 30 m. Most of the velocity profiles used earlier in this paper extend to depths considerably greater than 30 m, and we have taken advantage of this to look at the correlation of V_{S30} with V_{Sz} for depths as great as 600 m. The results for a representative

set of depths are shown in Figure 10. The figure shows that the correlation of V_{S30} with V_{Sz} is high even for depths many times 30 m. The correlations for the four regions are subjectively similar, at least for those depths reached by the velocity profiles in the various regions. Only the dataset from Japan has velocity profiles extending to depths of 200 m and greater. It is interesting to consider if the correlation for the other regions would be similar to that from Japan for the depths below the maximum depths for the profiles in each region. We can speculate on this for California, for which several studies have found an inverse correlation between V_{S30} and basin depths greatly exceeding 200 m (e.g., the references between basin depth and V_{S30} mentioned earlier in this paper, as well as figure 14 in Boore and Atkinson, 2008). This suggests that the correlation of V_{S30} with V_{Sz} for the Japanese data shown in Figure 10 might also hold for California data, at least qualitatively, with lower values of V_{S30} corresponding to lower values of V_{Sz} at a given depth.

Not surprisingly, the variability in V_{S30} for a given V_{Sz} increases with depth, at least up to about 150 m, but for greater depths the variability is approximately constant. We fit the equation

$$\log V_{Sz} = c_0 + c_1 \log V_{S30} \qquad (7)$$

to the KiK-net data (note that here we are interested in predicting V_{Sz} from V_{S30} for $z > 30$ m, rather than the other
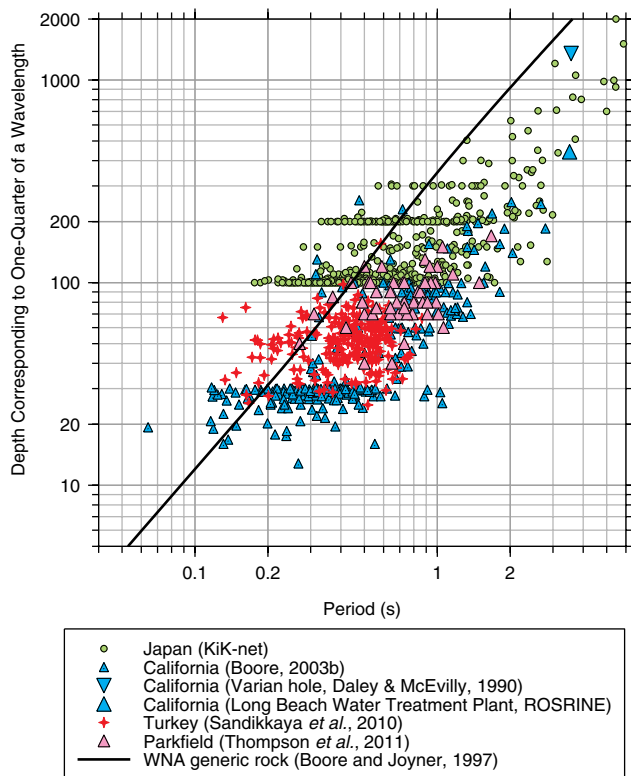
Figure 9. The depth that equals one-quarter of a wavelength of an *S* wave of the specified period traveling vertically in a uniform material with a velocity equal to the time-averaged velocity between the maximum depth of the profile and the surface. Each symbol represents the velocity profile at an individual site. For comparison, the black line shows the relation between depth and period for the generic rock shear-wave velocity profile of Boore and Joyner (1997) In addition to the California profiles referenced in the legend, we also used profiles for the Parkfield, California, region from Thompson *et al.* (2011). The color version of this figure is available only in the electronic edition.

way around, as earlier in this paper). Predicted values of V_{Sz} for a representative value of $V_{S30} = 300$ m/s are shown as a function of averaging depth in Figure 11, along with the standard deviation of the residuals to the fit and the number of points in the fit (a second-order polynomial gave similar results). Note that the small range of velocity values at greater depths (e.g., 600 m) makes it difficult to conclude much about the correlation between the velocities. However, the consistent trends of the predicted values of V_{Sz} suggest that the correlation of V_{Sz} and V_{S30} persists to depths in excess of several hundred meters. The correlation of V_{S30} with V_{Sz} shown in Figure 10 provides some justification for the use of V_{S30} as the site-response predictor variable in GMPEs for periods longer than several tenths of a second. Of course, it is possible that more accurate predictions of ground-motions can be made if the empirically based GMPEs used V_{Sz} with *z* commensurate with the oscillator period of interest. This requires a velocity profile extending to sufficient depths below each site providing ground-motion observations. To our

knowledge, the only GMPEs that use V_{Sz} with *z* different than 30 m are those of Joyner and Fumal (1985).

Summary and Discussion

The time-averaged shear-wave velocity to 30 m (V_{S30}), used as a proxy for site amplification in recent GMPEs and building codes, is strongly correlated with average velocities to depths less than and greater than 30 m (V_{Sz}, with *z* being the averaging depth). These correlations are both regionally dependent and network dependent; the KiK-net stations in Japan have systematically greater V_{S30} for a given V_{Sz} than for profiles from California, Turkey, and other sites in Europe. Furthermore, there are different trends in the velocity profiles for the KiK-net and K-NET stations within Japan. We attribute both the regional and network differences to be largely the result of siting criteria for the stations rather than regional differences in geology or geomorphology: the KiK-net sites were intended to be on rocklike materials because they are colocated with the High Sensitivity Seismograph Network (Hi-net) stations, whereas the velocity profiles used here from other regions are primarily from strong-motion sites in urban regions underlain by sediments. For the KiK-net velocity profiles, we provide equations relating V_{S30} to V_{Sz} for depths from 5 to 29 m in 1-m increments (the equations are in terms of the logarithms of the velocities, as we find that the velocities are consistent with a log-normal distribution). These equations can be used to estimate V_{S30} from V_{Sz} for sites in which velocity profiles do not extend to 30 m and for which there is reason to think that the velocity profile beneath the site is similar to that beneath KiK-net sites (the set of equations given in Boore, 2004b, can be used for sites underlain by lower-velocity materials). Two sets of equations are given, one set is to be used when nothing is known about the site classes, and the other set when NEHRP class E can be assigned to a site based on inspection of the site. Caution must be used in applying these equations to estimate V_{S30} at sites of the K-NET network in Japan, as a number of the sites seem to be on lower-velocity sediments than exist under KiK-net sites; in this case the equations of Boore (2004b) from California velocity profiles might be more appropriate for estimating V_{S30}. Our preferred estimates for V_{S30} at the K-NET sites comes from a linear weighted combination of the log V_{Sz} estimates from the KiK-net and the California velocity profiles.

The standard deviations of the residuals in the equations relating V_{S30} to V_{Sz} decreases with depth (for $z < 30$ m), but even for an averaging depth of 5 m an uncertainty of ±1 standard deviation in log V_{S30} (a factor of 1.7 in V_{S30}) maps into less than a 20% uncertainty in short-period ground motions predicted by recent GMPEs, although the sensitive of the ground motions to V_{S30} uncertainty is considerably larger at long periods (but is less than a factor of 1.2 for averaging depths greater than about 20 m).

We also find that V_{Sz} is correlated with V_{S30} for depths greater than several hundred meters, with the standard deviation of the scatter in log V_{Sz} for a given log V_{S30} being
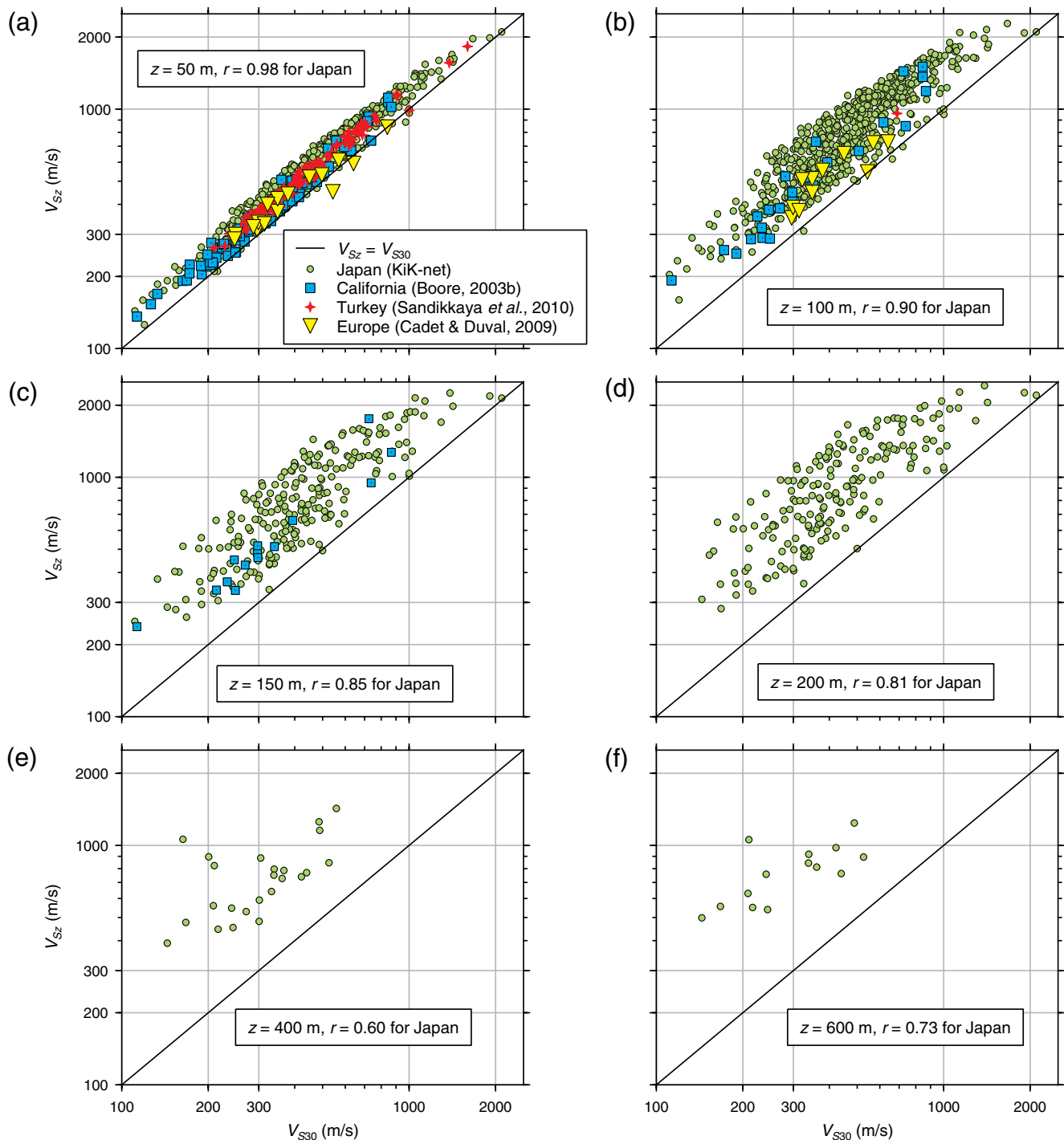
Figure 10. Correlation of V_{S30} and V_{Sz} from shear-wave velocity profiles for averaging depths z of 50, 100, 150, 200, 400, and 600 m (not all profiles extended to all depths, thus explaining the absence of points for all but the Japan profiles for the deeper depths). The Pearson correlation coefficient r between V_{Sz} and log V_{S30} for the Japan dataset is given in the comment box for each graph. The color version of this figure is available only in the electronic edition.

about 0.1 for z near 160 m; this is equivalent to the scatter in log V_{S30}, given log V_{Sz} at a depth of 5 m. This provides some justification for the use of V_{S30} as a proxy for site amplification for periods for which a quarter wavelength far exceeds 30 m. This does not invalidate efforts to improve site amplification estimates in GMPEs by adding information

about the depth of sediments or the presence of strong impedance contrasts (as inferred, for example, from the presence of resonant periods at sites). Even though there is a clear dependence of ground-motion amplification on V_{S30}, there is a large amount of variability in ground motions remaining after correcting for V_{S30}. An important task is
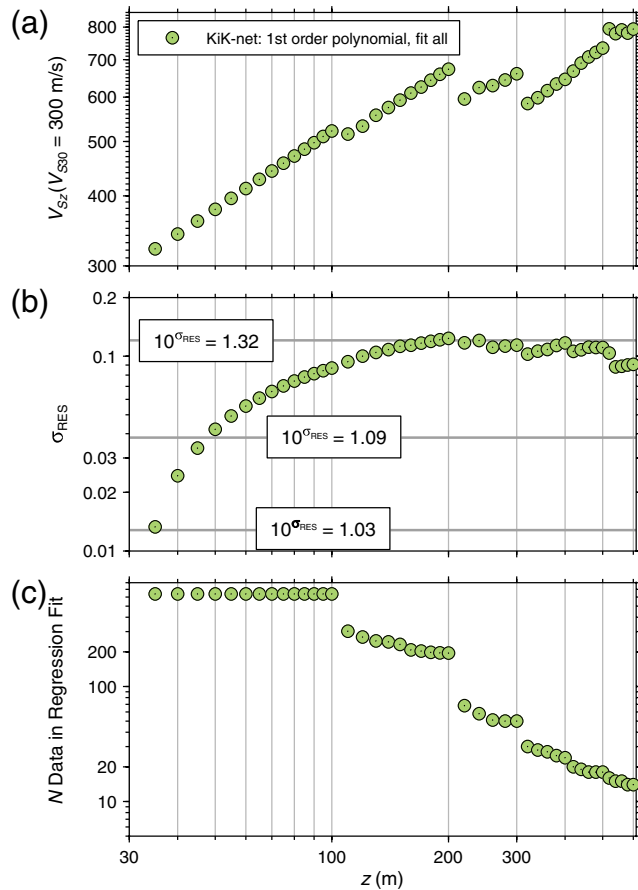
Figure 11. Some results of fitting V_{Sz} as a function of V_{S30} for KiK-net velocity profiles for averaging depths ranging from 35 to 600 m: (a) predicted V_{Sz} for $V_{S30} = 300$ m/s; (b) standard deviation of residuals; (c) number of points in the regression. The color version of this figure is available only in the electronic edition.

to reduce this variability by introducing other site-response variables that can be obtained without a large amount of time or expense, but this is beyond the scope of the present paper.

Data and Resources

The KiK-net velocity profiles came from ftp://ftp.kik .bosai.go.jp/pub/sitedat/ (last accessed July 2011); the K-NET velocity profiles were obtained from ftp://www. k-net.bosai.go.jp/knet/sitedat/ (last accessed July 2011). The California borehole velocity profiles are from a compendium by Boore (2003b), available from the online data section of www.daveboore.com (last accessed July 2011) . The ROSRINE velocity profiles were obtained from http://gees .usc.edu/ROSRINE/ (last accessed July 2011). The velocity profiles for the Turkish sites can be obtained from http:// daphne.deprem.gov.tr/2K/daphne_v4.php (last accessed July 2011). The PSA values in Figure 7 were computed using the Fortran program described in Kaklamanos et al. (2010).

References

Abrahamson, N. A., and W. J. Silva (2008). Summary of the Abrahamson & Silva NGA ground-motion relations, *Earthq. Spectra* **24,** 67–97.

Abrahamson, N., G. Atkinson, D. Boore, Y. Bozorgnia, K. Campbell, B. Chiou, I. M. Idriss, W. Silva, and R. Youngs (2008). Comparisons of the NGA ground-motion relations, *Earthq. Spectra* **24,** 45–66.

Allen, T. I., and D. J. Wald (2009). On the use of high-resolution topographic data as a proxy for seismic site conditions (V_{S30}), *Bull. Seismol. Soc. Am.* **99,** 935–943.

American Society of Civil Engineers (ASCE) (2010). *Minimum Design Loads for Buildings and Other Structures*, Standards ASCE/SEI 7-10, ISBN 9780784410851, 650 pp.; also available at http://www .asce.org/Product.aspx?id=2147487569,

Boore, D. M. (2003a). Prediction of ground motion using the stochastic method, *Pure Appl. Geophys.* **160,** 635–676.

Boore, D. M. (2003b). A compendium of P- and S-wave velocities from surface-to-borehole logging: Summary and reanalysis of previously published data and analysis of unpublished data, *U. S. Geol. Surv. Open-File Report 03-191*, 13 pp.

Boore, D. M. (2004a). Can site response be predicted? *J. Earthq. Eng.* **8,** no. 1, 1–41.

Boore, D. M. (2004b). Estimating $\bar{V}_S(30)$ (or NEHRP site classes) from shallow velocity models (depths < 30 m), *Bull. Seismol. Soc. Am.* **94,** 591–597.

Boore, D. M. (2006). Determining subsurface shear-wave velocities: A review, in *Third International Symposium on the Effects of Surface Geology on Seismic Motion*, P.-Y. Bard, E. Chaljub, C. Cornou, F. Cotton, and P. Gueguen (Editors), Laboratoire Central des Ponts et Chaussées, Grenoble, France, 30 August–1 September 2006, 67–85.

Boore, D. M., and G. M. Atkinson (2008). Ground-motion prediction equations for the average horizontal component of PGA, PGV, and 5%-damped PSA at spectral periods between 0.01 s and 10.0 s, *Earthq. Spectra* **24,** 99–138.

Boore, D. M., and W. B. Joyner (1997).Site amplifications for generic rock sites, *Bull. Seismol. Soc. Am.* **87,** 327–341.

Boore, D. M., W. B. Joyner, and T. E. Fumal (1994). Estimation of response spectra and peak accelerations from western North American earthquakes: An interim report, Part 2, *U.S. Geol. Surv. Open-File Report 94-127*, 40 pp.

Boore, D. M., W. B. Joyner, and T. E. Fumal (1997). Equations for estimating horizontal response spectra and peak acceleration from western North American earthquakes: A summary of recent work, *Seismol. Res. Lett.* **68,** 128–153.

Bragato, P. L. (2008). Limits for the improvement of ground-motion relations in Europe and the Middle East by accounting for site effects, *Bull. Seismol. Soc. Am.* **98,** 2061–2065.

Building Seismic Safety Council (2003). *Recommended Provisions for Seismic Regulations for New Buildings and Other Structures, Part 1: Provisions.* Report No. FEMA-450, Federal Emergency Management Agency, Washington, D.C., 303 pp

Cadet, H., and A.-M. Duval (2009).A shear wave velocity study based on the KiK-net borehole data: A short note, *Seismol. Res. Lett.* **80,** 440–445.

Campbell, K. W., and Y. Bozorgnia (2008). NGA ground motion model for the geometric mean horizontal component of PGA, PGV, PGD and 5% damped linear elastic response spectra for periods ranging from 0.01 to 10 s, *Earthq. Spectra* **24,** 139–171.

Castellaro, S., F. Mulargia, and P. L. Rossi (2008) .V_{S30}: Proxy for seismic amplification? *Seismol. Res. Lett.* **79,** 540–543.

Cauzzi, C., and E. Faccioli (2008). Broadband (0.05 to 20 s) prediction of displacement response spectra based on worldwide digital records, *J. Seismol.* **12,** 453–475.

Chiou, B. S. J., and R. R. Youngs (2008). An NGA model for the average horizontal component of peak ground motion and response spectra, *Earthq. Spectra* **24,** 173–215.

Choi, Y., and J. P. Stewart (2005). Nonlinear site amplification as function of 30 m shear wave velocity, *Earthq. Spectra* **21,** 1–30.

Daley, T. M., and T. V. McEvilly (1990). Shear-wave anisotropy in the Parkfield Varian well VSP, *Bull. Seismol. Soc. Am.* **80,** 857–869.

Day, S. M. (1996). RMS response of a one-dimensional halfspace to *SH*, *Bull. Seismol. Soc. Am.* **96,** 363–370.

Dobry, R., R. D. Borcherdt, C. B. Crouse, I. M. Idriss, W. B. Joyner, G. R. Martin, M. S. Power, E. E. Rinne, and R. B. Seed (2000). New site coefficients and site classification system used in recent building seismic code provisions, *Earthq. Spectra* **16,** 41–67.

Douglas, J., P. Gehl, L. F. Bonilla, O. Scotti, J. Régnier, A.-M. Duval, and E. Bertrand (2009). Making the most of available site information for empirical ground-motion prediction, *Bull. Seismol. Soc. Am.* **99,** 1502–1520. doi 10.1785/0120080075.

Eurocode 8 (2004). Design of structures for earthquake resistance, part 1: General rules, seismic actions and rules for buildings, EN 1998-1, European Committee for Standardization (CEN), http://www.cen.eu/cenorm/homepage.htm (last accessed July 2011).

Figini, R. (2006). Analisi degli effetti di sito sui lunghi periodi degli spettri di risposta di spostamento, *Master's Thesis*, Politecnico di Milano.

Joyner, W. B., and T. E. Fumal (1985). Predictive mapping of earthquake ground motion, in *Evaluating Earthquake Hazards in the Los Angeles Region* J. I. Ziony (Editor), *U.S. Geol. Surv. Profess. Paper 1360*, 203–220.

Joyner, W. B., R. E. Warrick, and T. E. Fumal (1981). The effect of Quaternary alluvium on strong ground motion in the Coyote Lake, California, earthquake of 1979, *Bull. Seismol. Soc. Am.* **71,** 1333–1349.

Kaklamanos, J., D. M. Boore, E. M. Thompson, and K. W. Campbell (2010). Implementation of the Next Generation Attenuation (NGA) ground-motion prediction equations in FORTRAN and R, *U. S. Geological Survey Open-File Report 2010-1296*, 47 pp

Kanno, T., A. Narita, N. Morikawa, H. Fujiwara, and Y. Fukushima (2006). A new attenuation relation for strong ground motion in Japan based on recorded data, *Bull. Seismol. Soc. Am.* **96,** 879–89.

Kinoshita, S. (1998). Kyoshin-net (K-NET), *Seismol. Res. Lett.* **69,** 309–332.

Lee, V. W., and M. D. Trifunac (2010). Should average shear-wave velocity in the top 30m of soil be used to describe seismic amplification?, *Soil Dynam. Earthq. Eng.* **30,** 1250–1258.

Moss, R. E. S. (2008). Quantifying measurement uncertainty associated with thirty meter shear wave velocity (V_{S30}), *Bull. Seismol. Soc. Am.* **98,** 1399–1411.

Moss, R. E. S. (2011). Reduced sigma of ground-motion prediction equations through uncertainty propagation, *Bull. Seismol. Soc. Am.* **101,** 250–257.

Mucciarelli, M, and M. R. Gallipoli (2006). Comparison between V_{S30} and other estimates of site amplification in Italy, Paper No. 270, *First European Conference on Earthquake Engineering and Seismology, a Joint Event of the 13th European Conference on Earthquake Engineering and 30th General Assembly of the European Seismological Commission*, Geneva, Switzerland, 3–8 September 2006, available from http://www.earth-prints.org/handle/2122/1945 (last accessed July 2011).

Okada, Y., K. Kasahara, S. Hori, K. Obara, S. Sekiguchi, H. Fujiwara, and A. Yamamoto (2004). Recent progress of seismic observation networks in Japan-Hi-net, F-net, K-NET and KiK-net, *Earth Planets Space* **56,** xv–xxviii.

Sandıkkaya, M. A., M. T. Yılmaz, B. S. Bakır, and Ö. Yılmaz (2010). Site classification of Turkish national strong-motion stations, *J. Seismol.* **14,** 543–563.

Thompson, E. M., L. G. Baise, R. E. Kayen, E. C. Morgan, and J. Kaklamanos (2011). Multiscale site-response mapping: A case study of Parkfield, California, *Bull. Seismol. Soc. Am.* **101,** 1081–1100.

Wald, D. J., and T. I. Allen (2007). Topographic slope as a proxy for seismic site conditions and amplification, *Bull. Seismol. Soc. Am.* **97,**1379–1395.

U.S. Geological Survey
MS 977, 345 Middlefield Road
Menlo Park, California 94025
boore@usgs.gov
(D.M.B.)

Tufts University
113 Anderson Hall
Medford, Massachusetts 02155
eric.thompson@tufts.edu
(E.M.T.)

ISTerre (Institut des Sciences de la Terre)
BP 53
38041 Grenoble, cedex 9
France
hcadet@obs.ujf-grenoble.fr
(H.C.)